Atmospheric Research 218 (2019) 296–305

Contents lists available at ScienceDirect

Atmospheric Research

journal homepage: www.elsevier.com/locate/atmosres

Population exposed to drought under the 1.5 °C and 2.0 °C warming in the Indus River Basin

Shanshan Wen[a], Anqian Wang[b,e,**], Hui Tao[b], Khalid Malik[d], Jinlong Huang[a], Jianqing Zhai[a,c], Cheng Jing[b,e], Ghulam Rasul[d], Buda Su[a,b,*]

[a] Collaborative Innovation Center on Forecast and Evaluation of Meteorological Disasters, Institute for Disaster Risk Management, School of Geographical Science, Nanjing University of Information Science & Technology, Nanjing 210044, China
[b] Institute of Ecology and Geography, Chinese Academy of Sciences, State Key Laboratory of Desert and Oasis Ecology, Xinjiang 830011, China
[c] China Meteorological Administration, National Climate Center, Beijing 10081, China
[d] Pakistan Meteorological Department, Islamabad 44000, Pakistan
[e] University of Chinese Academy of Sciences, Beijing 100049, China

ARTICLE INFO

Keywords:
Drought
Population Exposure
Intensity-Area-Duration
Shared Socioeconomic Pathways
Indus River Basin

ABSTRACT

Based on multiple global climate models (GCMs), the Standardized Precipitation Evapotranspiration Index (*SPEI*) and Intensity-Area-Duration (IAD) method were used to identify drought events of the Indus River Basin (IRB) in the reference period (1986–2005) and under 1.5 °C (2020–2039 in RCP2.6) and 2.0 °C (2040–2059 in RCP4.5) global warming scenarios. Then, the population exposure was assessed by combining drought events with a projected dynamic population amount from five Shared Socioeconomic Pathways (SSPs), in which describe future of societal development considering the effects of climate change and climate policies. Research results show that both precipitation and evapotranspiration are projected to increase with global warming. Due to a higher increase in evapotranspiration than in precipitation, frequency, intensity, and areal coverage of drought events in the IRB are expected to increase under the 1.5 °C and 2.0 °C warming scenarios relative to the 1986–2005 reference period. In particular, frequency and areal coverage of extreme severe droughts will increase significantly. With aggravation of droughts across the IRB, annual population exposure will increase considerably from 43.2 million in 1986-2005 to approximately 114.4 million based on SSP1 (a sustainable world) under the 1.5 °C global warming scenario and will reach 163.1 million based on SSP3 (a strongly fragmented world) under the 2.0 °C scenario. Compared with the 2.0 °C level, maintaining the increase in global average temperature below the 1.5 °C limit can reduce the population exposed to drought by approximately 1.4-fold.

1. Introduction

As one of the most complicated and recurring natural hazards, droughts impact social, economic, ecological, and cultural aspects in almost all of the climate belts, especially in rain-fed agricultural regions with varying frequency, severity, and duration (Trenberth et al., 2014; Deo and Sahin, 2015; Kelley et al., 2015; Deo et al., 2017; Su et al., 2018; Byakatonda et al., 2018). Enhanced drying has been observed and projected over many regions under a warming climate, which is attributable to increasing atmospheric concentrations of greenhouse gases. Drought frequency is projected to increase in the coming decades, and humans' exposure to water scarcity is likely to increase simply because of population growth and climate change (Watts et al., 2015). Understanding the spatial and temporal characteristics of droughts is of importance for mitigating adverse impacts of drought risks, especially in vulnerable regions (Mishra and Singh, 2010; He et al., 2011; Zhai et al., 2016). Located in South Asia, the Indus River is the main source of water resources for Pakistan, Afghanistan and India. These countries have experienced an increase in severe climate extremes and are thus highly vulnerable to climate change (Schilling et al., 2013; Su et al., 2016; Huang et al., 2017). For instance, droughts affected 3.3 million people and resulted in a negative growth of 2.6% in

* Corresponding author at: Collaborative Innovation Center on Forecast and Evaluation of Meteorological Disasters, Institute for Disaster Risk Management, School of Geographical Science, Nanjing University of Information Science & Technology, Nanjing 210044, China.
** Corresponding author at: Institute of Ecology and Geography, Chinese Academy of Sciences, State Key Laboratory of Desert and Oasis Ecology, Xinjiang 830011, China.
E-mail addresses: wangaq1990@163.com (A. Wang), subd@cma.gov.cn (B. Su).

https://doi.org/10.1016/j.atmosres.2018.12.003
Received 26 December 2017; Received in revised form 28 November 2018; Accepted 3 December 2018
Available online 04 December 2018
0169-8095/ © 2018 Elsevier B.V. All rights reserved.

the Pakistani agricultural sector in 2002 (Ahmad et al., 2004). More than 300 million people were affected by severe drought events in 2002 and 2014 in India (Barthel and Neumayer, 2012; Mishra et al., 2016), and the severe droughts in 2017 in South India affected > 0.2 million people (Aadhar and Mishra, 2017).

To address the adverse impacts of a warming climate, the Paris Agreement proposed to maintain the increase in global mean temperature to well below 2.0 °C above pre-industrial level and to strive for 1.5 °C (UNFCCC, 2015). Since then, significant efforts have been devoted to analyze the different climatic impacts of 1.5 and 2.0 °C warming (Schleussner et al., 2016a; Mitchell et al., 2016; Hulme, 2016; King et al., 2017; Su et al., 2018; Zhang et al., 2018). The Special Report on Global warming of 1.5 °C (SR15) concluded that 1.5 °C warming will bring severe impacts on terrestrial and marine ecosystems, human health, food and water security, and socioeconomic development, but negative impacts of 1.5 °C warming on natural and human systems are lower compared to 2.0 °C warming. At a global scale, the average monthly number of people projected to be exposed to extreme droughts at the 1.5 °C level will be 114.3 million in 2021–2040 and will further increase to 190.4 million and more than double the current status at the 2.0 °C by 2041–2060 (Hoegh-Guldberg et al., 2018). At a regional scale, exposure of the population to droughts in the Haihe River Basin, China, in a warming world quantified by the regional climate model CCLM found that exposure will decrease slightly at the 1.5 °C level under the assumption that the population hold constant at the 1986–2005, even though a substantial increase is projected at the 2.0 °C warming (Sun et al., 2017). However, a most recent study on the population exposure in China shows that 413.9 million people will be exposed to droughts at 1.5 °C global warming, from 401.0 million in 1986–2005, under a dynamic population scenario (Chen et al., 2018).

The population and economy change over time, and results derived from a fixed socioeconomic scenario are not robust enough to support decision making (Smirnov et al., 2016). Therefore, five Shared Socioeconomic Pathways (SSPs) have been developed to describe a set of plausible alternative futures of societal development considering the effects of climate change and climate policies over the 21st century. Specifically, SSP1, SSP2, and SSP3 refer to low, intermediate and high challenges, respectively, to mitigation and adaptation; SSP4 and SSP5 denote dominating adaptation challenges and dominating mitigation challenges, respectively. The SSPs represent sustainability (SSP1), a pathway of continuing historical trends (SSP2), fragmentation (SSP3), inequality (SSP4), and a growth-oriented world (SSP5) (O'Neill et al., 2014; O'Neill et al., 2017).

The current study presents characteristics of drought events and the population exposed to droughts in the Indus River Basin (IRB) under 1.5 °C and 2.0 °C global warming, based on multiple GCM outputs and the demographic prediction of five SSPs. Since drought events are a spatial-temporal process with certain intensity, spatial extent, and duration (Sheffield and Wood, 2007; Xu et al., 2015), the Intensity-Area-Duration (IAD) method, which provides a 3-dimensional perspective to describe extreme events (Zhai et al., 2016; Huang et al., 2018), is used to analyze drought events in the study. The main target of this paper is to provide regional evidence on the impacts resulting from an extra 0.5 °C warming by assessing the feature and influence of drought events, so as to support policymakers in the development of climate change adaptation and mitigation strategies.

2. Study area and data

Located between 22°~38°N and 65°~83°E in South Asia, the Indus River Basin (IRB) covers an area of approximately 1.1 million km^2, and China, Afghanistan, Pakistan, and India share the basin (Fig. 1). The Indus River originates from the Tibetan Plateau, flows northwest through the western Himalayan Mountains and finally enters the Arabian Sea. The upper Indus River flows from its origin to Kalabagh, and downstream of Kalabagh is composed of plain and desert. The basin is mainly recharged by monsoon rainfall and glacier-snow melting water.

As meteorological stations are mainly located in the lower elevation zone, precipitation in the mountainous upper basin is usually underestimated. For comparison, two reanalysis series were used to evaluate the performance of climate models in reproducing the regional climate in the IRB. The Asian Precipitation-Highly-Resolved Observational Data Integration Towards Evaluation of Water Resources (APHRODITE) project generated daily precipitation time series for 1951–2007 at a 0.5° × 0.5° resolution based on dense rain-gauge data from thousands of Asian stations (Yatagai et al., 2012) and was evaluated as the best

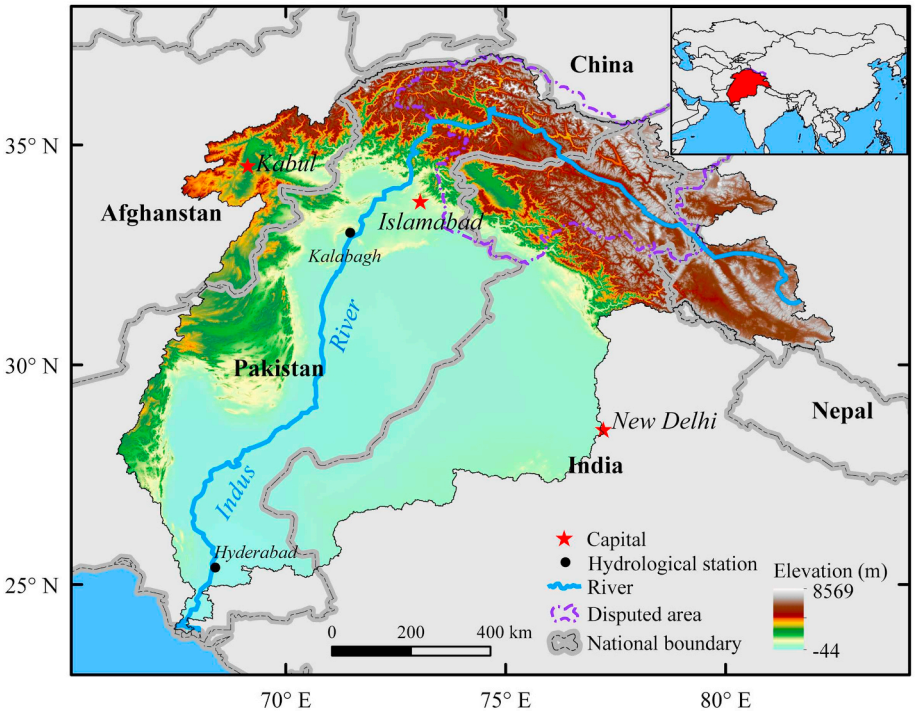

Fig. 1. Location of the Indus River Basin.

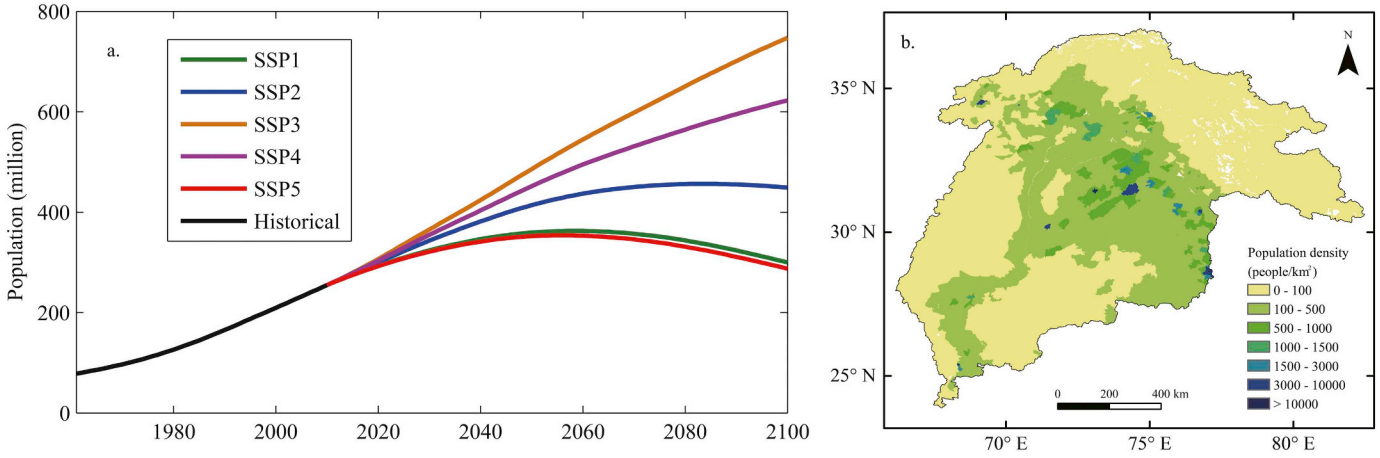

Fig. 2. Time series of population in the Indus River Basin: historical period (1961–2010) and projected period (2010–2099) under SSPs (a), and spatial distribution of population in 2010 (b).

precipitation estimate over Asia (Andermann et al., 2011; Rajbhandari et al., 2014; Ghajarnia et al., 2015; Su et al., 2016). The latest Climatic Research Unit dataset (CRU TS v4.01), which contains monthly precipitation, daily maximum and minimum temperature, and other climate variables for 1901–2016 at a spatial resolution of 0.5° × 0.5°, is based on > 4000 individual weather stations around the world (Harris et al., 2014).

Climate outputs from five GCMs, namely, GFDL-ESM2M, HadGEM2-ES, IPSL-CM5A-LR, MIROC-ESM-CHEM, and NorESM1-M, under four RCP scenarios (RCP 2.6, 4.5, 6.0, and 8.5), are used in this study to project droughts in the IRB. GCM outputs include daily temperature, precipitation, air pressure, surface radiation, near-surface wind speed, and near-surface relative humidity from 1950 to 2099 and have been downscaled to 0.5° × 0.5° resolution and bias corrected to ensure statistical agreement with the observational data (Hempel et al., 2013; Warszawski et al., 2014).

National level population datasets for 1960–2016 were obtained from the World Bank, and for 2010–2100 under different SSPs from the International Institute for Applied Systems Analysis (IIASA). SSPs assume that the population will maintain its current trend based on SSP2; will have low fertility, low mortality, medium migration, and high education based on SSP1; medium fertility, medium mortality, medium migration, and medium education based on SSP3; high fertility, high mortality, medium migration, and polarized education based on SSP4; and low fertility, low mortality, high migration, and high education based on SSP5 (Kc and Lutz, 2017).

The gridded population of the world, version four (GPWv4) (Center for International Earth Science Information Network - CIESIN - Columbia University, 2016) contains the distribution of the population on a continuous global surface (Tobler et al., 1997). In this study, the current grid size of 30 arc *sec* in the GPWv4 product was re-sampled to 0.5° × 0.5° to match the climate outputs. The proportion of the population in each grid to the national total in 2010 from GPWv4 was used to deduce gridded population under SSPs in China, Afghanistan, Pakistan, and India for the period 2010–2100. The recorded and projected population in the IRB for the periods 1961–2010 and 2010–2100 and the distribution of population in 2010 are shown in Fig. 2.

3. Methodology

3.1. Standardized precipitation evapotranspiration index (SPEI)

The Standardized Precipitation Evapotranspiration index (*SPEI*) can describe the extent to which dry and wet conditions deviate from the long-term average by standardizing the difference between potential evapotranspiration and precipitation. The *SPEI*-12 used in this paper reflects the long-term water loss process and indicates the inter-annual change of droughts. The calculation of *SPEI* is briefly described as follows:

(1) Potential evapotranspiration (PET) is estimated by the Penman-Monteith (PM) method:

$$PET = \frac{0.408\Delta(R_n - G) + \gamma\frac{900}{T+273}u_2(e_a - e_d)}{\Delta + \gamma(1 + 0.34u_2)}, \quad (1)$$

where PET is the daily potential evapotranspiration (mm·d^{-1}); Δ is the slope of the saturation vapor pressure curve (kPa·°C^{-1}); T is the mean daily air temperature (°C); e_a is the saturation vapor pressure (kPa); R_n is the net radiation at the surface (MJ/(m^2·d)); e_d is the actual atmospheric water vapor pressure (kPa); G is the all-wave ground heat flux (MJ/(m^2·d)); γ is the psychometric constant (kPa·°C^{-1}); and u_2 is the daily average wind speed at a height of 2 m (m·s^{-1}).

(2) The accumulated difference between the precipitation and PET is normalized by a three-parameter log-logistic probability distribution:

$$F(X) = \left[1 + \left(\frac{\alpha}{X - \gamma}\right)^{\beta}\right]^{-1}, \quad (2)$$

where x is the accumulated difference between the precipitation and PET; α, β and γ are scale, shape and position parameters, respectively. Then, *SPEI* can be deduced by:

$$SPEI = w - \frac{C_0 + C_1 w + C_2 w^2}{1 + d_1 w + d_2 w^2 + d_3 w^3} \left(w = \sqrt{-2\ln p}, \text{If} \leq 0.5\right), \quad (3)$$

$$SPEI = \frac{C_0 + C_1 w + C_2 w^2}{1 + d_1 w + d_2 w^2 + d_3 w^3} - w \left(w = \sqrt{-2\ln(1-p)}, \text{If } p > 0.5\right), \quad (4)$$

where p is the probability of a given x; $C_0 = 2.515517$; $C_1 = 0.802853$; $C_2 = 0.010328$; $d_1 = 1.432788$;$d_2 = 0.189269$;$d_3 = 0.001308$ (Vicente-Serrano et al., 2010). -1 < *SPEI* < 1 denotes a near-normal condition; *SPEI* ≤ −1, −1.5 and −2 denote a moderate, severe, and extreme severe drought, respectively.

3.2. Intensity-Area-Duration method

A drought event can be defined from a 3-dimensional perspective by considering not only the event intensity and duration but also its spatial extent. In this study, the Intensity-Area-Duration (IAD) method is used to spatially cluster regions with similar drought conditions. The grid with the highest drought intensity (lowest *SPEI* value) is identified as the drought center first, and then, the adjacent grids that meet the criteria of $SPEI \leq -1$ are attached to the drought center sequentially. The processes will be iterated until no any adjacent grid meets the drought criteria. The summed area of clustered grids is the areal coverage of a drought event, and average *SPEI* over the summed area is the intensity of a drought event. Only the events with areal coverage larger than 25,000 km^2 are considered in the current drought study.

3.3. Definition of 1.5 °C and 2.0 °C global warming

The global mean temperature for 1986–2005 was 0.61 °C warmer than that in the pre-industrial period of 1850–1900 (IPCC, 2013); thus, further warming of 0.89 °C and 1.39 °C indicates the 1.5 °C and 2.0 °C warming limits, respectively. According to the ensemble mean of multiple GCMs, the 20-year running average of global mean temperatures will be 1.5 °C warmer than the pre-industrial value during the 2020–2039 period under the RCP 2.6 scenario and will be 2.0 °C warmer in the 2040–2059 period under the RCP 4.5 scenario (Warszawski et al., 2014; Schleussner et al., 2016b; Chen et al., 2017; Su et al., 2017; Su et al., 2018; Sun et al., 2018).

4. Results

4.1. Comparison between GCM simulation and observation

The inner-annual variations of GCM-simulated temperature and precipitation over the IRB for the period 1961–2005 are compared with the observational data in Fig. 3. The figure shows that GCMs quite accurately captured the monthly variation of temperature in the IRB, with lower temperature in winter (DJF) and higher in summer (JJA). The ensemble mean temperature is slightly higher than that from observations, but the deviation for each month is < 1.0 °C (Fig. 3a). The inner-annual variation of precipitation in the IRB is also well captured by the GCMs. The GCM ensemble overestimates precipitation, but deviations of monthly precipitation are < 5 mm except in July and August (Fig. 3b).

Spatial distribution patterns of GCM ensemble mean and observed annual mean temperature for the period 1961–2005 are compared in Fig. 4a-b. The geographical distribution feature of temperature in the IRB is well captured by the GCMs, with the annual mean temperature highest in the southeast but lowest in the northeast, and the spatial correlation coefficient of the simulated and observed temperature reaches 0.97 (significant at the 0.01). With respect to the distribution of annual precipitation, GCMs capture the spatial characteristics of higher than 1000 mm in the mountain fringe but < 500 mm in most other parts. The spatial correlation coefficient of simulated and observed precipitation is approximately 0.92 (significant at the 0.01 level) (Fig. 4c-d).

4.2. Projected precipitation and evapotranspiration

Both precipitation and evapotranspiration influence drought conditions. Changes in precipitation and evapotranspiration at the 1.5 °C and 2.0 °C warming levels relative to the reference period are presented in Fig. 5.

In the reference period, the areal averaged annual precipitation in the IRB is approximately 441.2 mm according to the ensemble mean, with a model range of 393.1–465.1 mm. Under the 1.5 °C warming scenario, precipitation will be 450.4 mm (range of GCMs: 397.0–505.0 mm), and 71.3% of the basin is projected to increase relative to the reference period. The largest increase of 80 mm occurs in the southeast, but a weak decrease in precipitation in the west and the mountain fringe in the IRB are projected. Under 2.0 °C warming, the areal averaged annual precipitation in the IRB is projected to be about 451.1 mm (390.0–548.5 mm), similar to that under the 1.5 °C warming scenario. Precipitation across 61.1% of the basin will increase relative to the reference period, and significant increases will be in the central IRB with the maximum of about 100 mm. A decrease in precipitation is projected to occur in the west and the mountain fringe, with the largest decrease of about 48 mm in the northwestern basin.

Potential evapotranspiration was approximately 1500.3 mm (1364.6–1568.4 mm) for 1986–2005 and gradually decreased from the southwest to the northeast of the basin. In the upper IRB, potential evapotranspiration is < 1000 mm but exceeds 2000 mm in the lower IRB. Potential evapotranspiration is projected to increase in the entire basin with warming. Under the 1.5 °C and 2.0 °C scenarios, potential evapotranspiration might increase to 1538.0 mm (1382.9–1625.6 mm) and 1558.4 mm (1383.8–1649.9 mm), respectively, over the IRB.

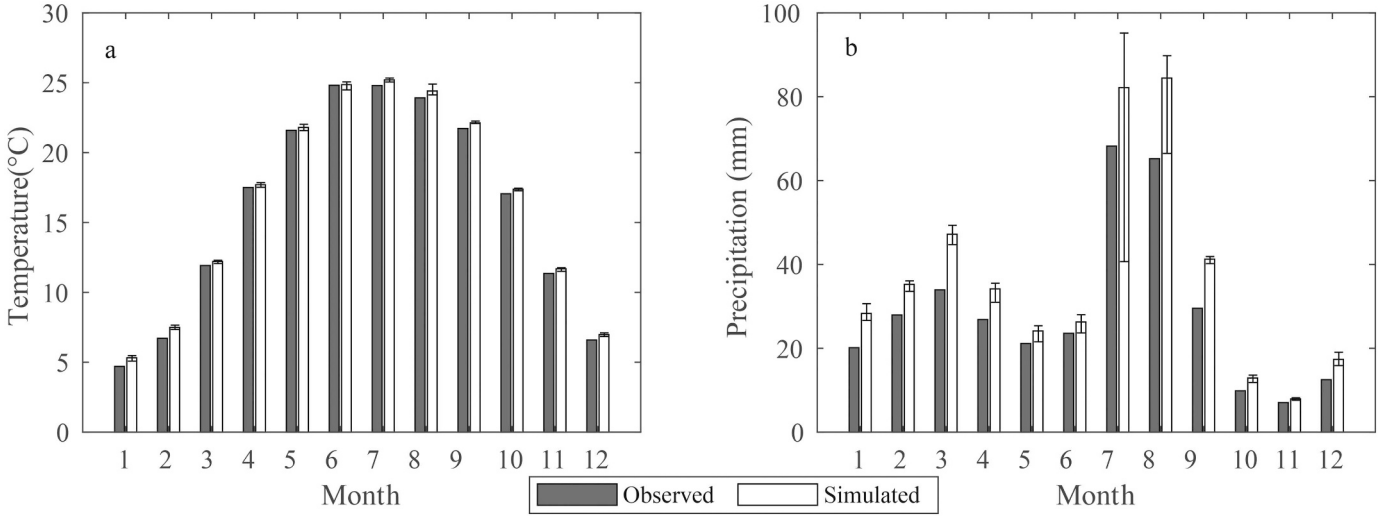

Fig. 3. Comparison of the GCM ensemble with observed data in the Indus River Basin during 1961–2005: multi-year averaged monthly temperature (a) and precipitation (b). Vertical lines denote the ranges of the GCMs.

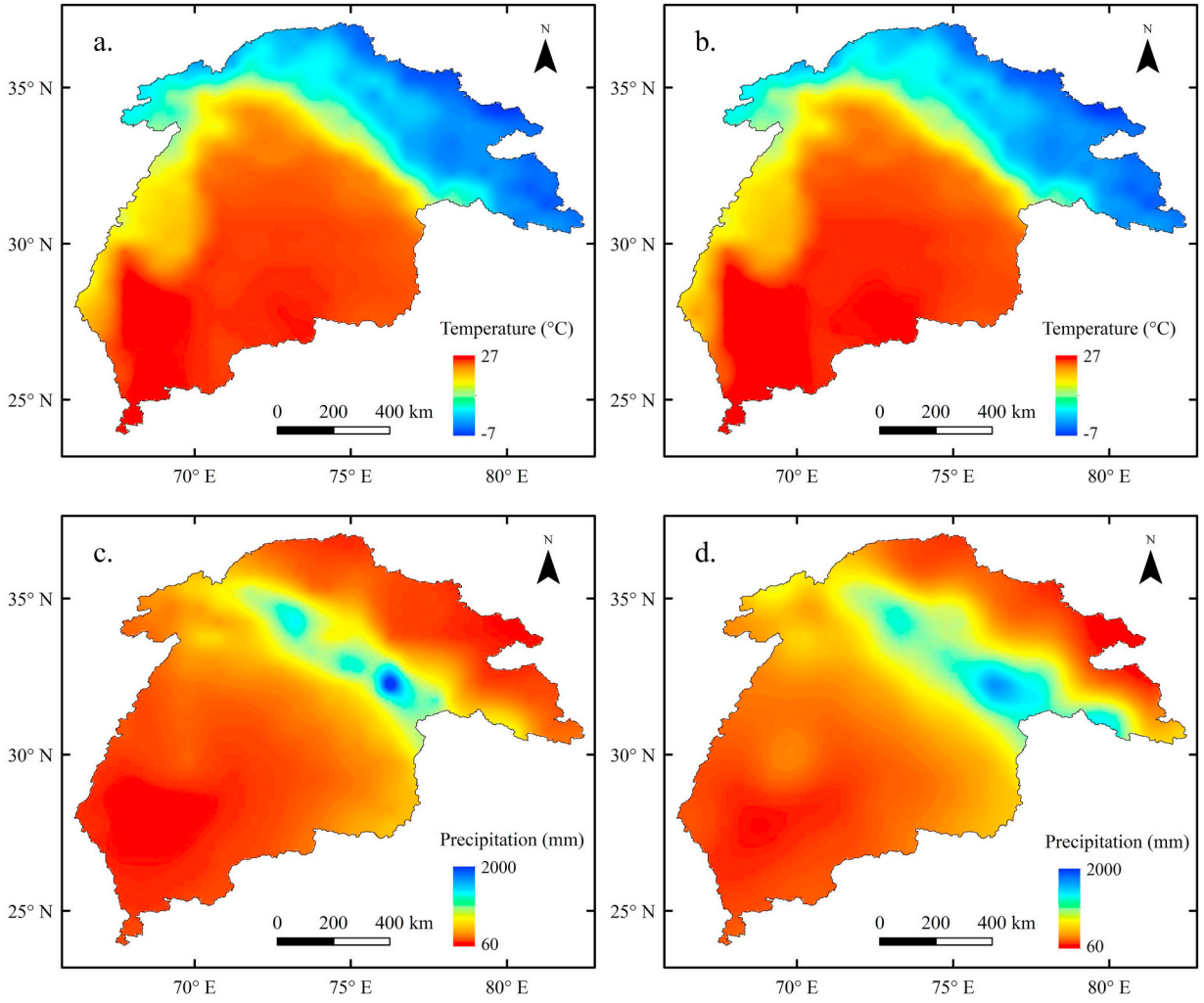

Fig. 4. Spatial distribution of observed and simulated annual mean temperature (a, b) and annual precipitation (c, d) for the 1961–2005.

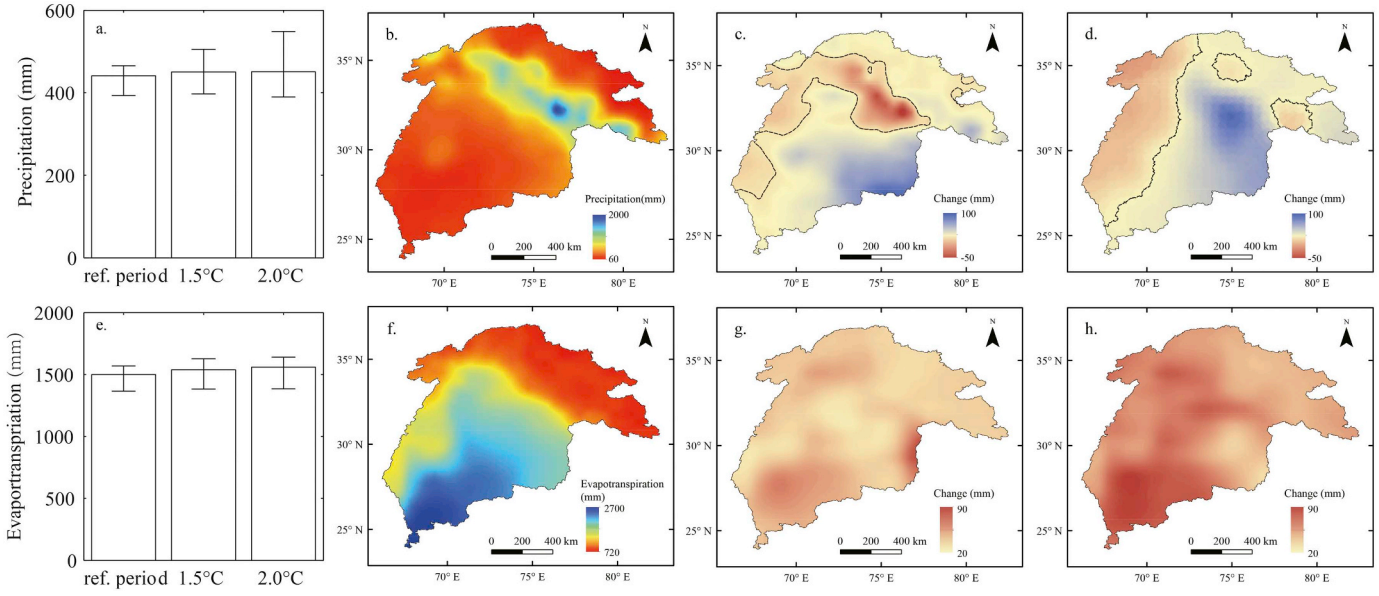

Fig. 5. Comparison of precipitation (a) and evapotranspiration (e) in the reference period and the warming world in the Indus River Basin; (b) and (f) show the spatial distribution of precipitation and evapotranspiration in the reference period; (c-d) and (g-f) are changes in precipitation and evapotranspiration at the 1.5 °C and 2.0 °C levels relative to the reference period. Vertical lines in (a) and (e) denote the range of the GCMs; dashed lines in (c) and (d) denote the 0 isolines.

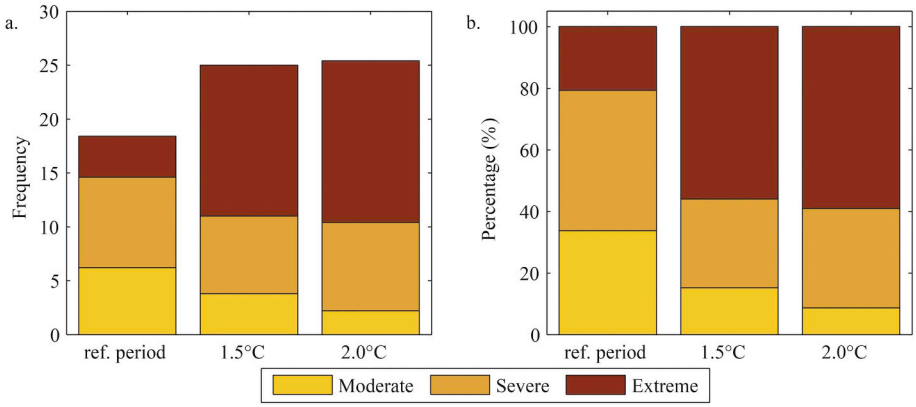

Fig. 6. Frequency of drought events with different magnitudes (a) and their percentages relative to total events (b) in the reference period and under the 1.5 °C and 2.0 °C warming.

4.3. Projected drought frequency, intensity and areal coverage

There were 18.4 drought events during 1986–2005 based on the ensemble mean of GCMs, with percentages of moderate, severe and extreme severe events accounting for 33.7%, 45.7%, and 20.6%, respectively (Fig. 6). Under the 1.5 °C warming scenario from 2020 to 2039, total drought events will be approximately 25, with moderate, severe, and extremely severe drought account droughts accounting for 15.2%, 28.8% and 56.0%, respectively. Under 2.0 °C warming, the drought frequency will be approximately 25.4 during 2040–2059, with the percentage of moderate, severe, and extremely severe droughts accounting for about 8.6%, 32.3%, and 59.1%, respectively. Extremely severe droughts will increase considerably with warming.

The spatial distribution of drought frequency during 1986–2005 in the IRB and changes relative to the reference period in the 1.5 °C and 2.0 °C warming levels are shown in Fig. 7. In the 20 years of the reference period, drought events occurred 3–5 times in the northern part, and > 5 times in most of the central and south parts. Under the 1.5 °C warming scenario, drought frequency in the entire basin will increase with the largest increase of > 80% in the north relative to the reference period. Under an additional 0.5 °C warming, drought frequency is projected to decrease about 10% in the east IRB relative to the reference period, but will increase by > 40% in the central part and by > 100% in the southern and northern IRB.

The intensity of total droughts and that of moderate, severe, and extreme severe droughts under the 1.5 °C and 2.0 °C warming levels and the reference period in the IRB is shown in Fig. 8. The *SPEI* averaged for all events was approximately −1.70 (range of GCMs: −1.87∼ − 1.55) for 1986–2005, and will be −2.03 (−2.28∼ − 1.74) under 1.5 °C and will further strengthen to −2.12 (−2.38∼ − 1.91) under 2.0 °C warming. It was projected that the intensity of moderate droughts will increase slightly at 1.5 °C but decrease at the 2.0 °C with relative to the reference period, while that of severe droughts exhibits no change at 1.5 °C but increases under 2.0 °C global warming. The intensity of extreme severe droughts will increase slightly under both the 1.5 °C and 2.0 °C warming relative to the reference period.

The areal coverage of drought events, including moderate, severe, and extremely severe droughts under the 1.5 °C and 2.0 °C warming levels and the reference period in the IRB are shown in Fig. 9. Annual drought affected an area of 260.4 thousand km^2 during 1986–2005 and is projected to increase to 394.0 thousand km^2 under the 1.5 °C warming scenario and to 406.9 thousand km^2 under the 2.0 °C scenario. In contrast, 36.2 thousand km^2 of moderate droughts in the reference period will decrease to 23.4 and 9.6 thousand km^2 annually under the 1.5 °C and 2.0 °C scenarios, respectively. Annual areal coverage of severe events will decrease from 118.9 thousand km^2 in the reference period to 88.3 thousand km^2 under 1.5 °C and 88.2 thousand km^2 under 2.0 °C. Unlike the trends of moderate and severe droughts, areal coverage of extreme severe droughts will increase significantly with warming.

4.4. Population exposed to droughts

Among the combinations of the four Representative Concentration Pathways (RCPs) and five Shared Socioeconomic Pathways (SSPs), some are unlikely to occur (van Vuuren et al., 2014). Considering the different mitigation and adaptation challenges assumed by SSPs, RCP2.6 is combined with SSP1 and SSP4, which will face a lower challenge of mitigation in the future when studying the impacts of 1.5 °C global warming, and RCP4.5 is combined with SSP2, SSP3, and

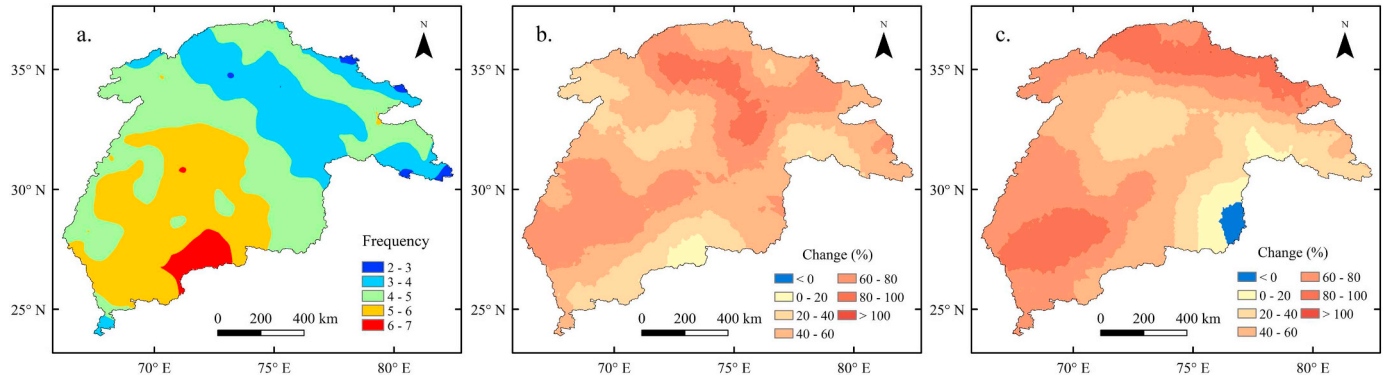

Fig. 7. Spatial distribution of drought frequency in the Indus River Basin for the 1986–2005 period (a), changes of drought frequency under 1.5 °C and 2.0 °C warming relative to the 1986–2005 period (b-c).

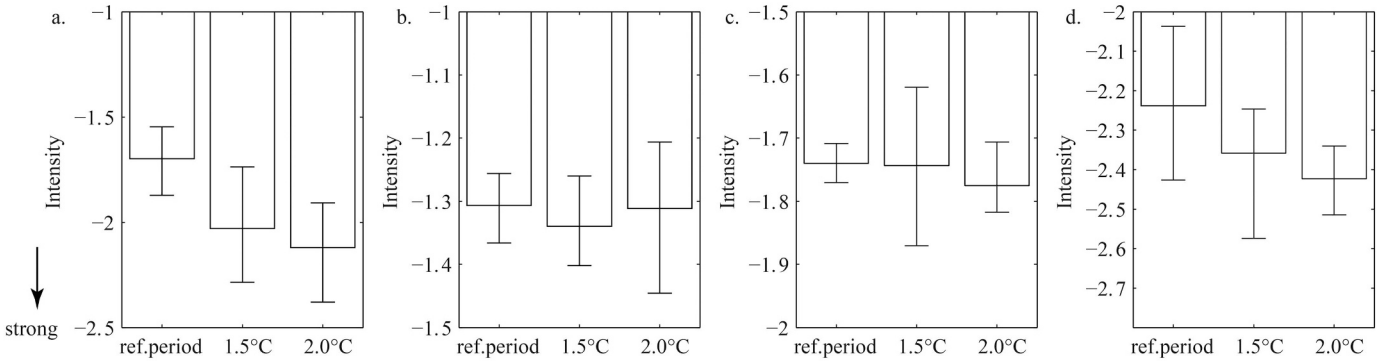

Fig. 8. Comparison of drought intensity with different magnitudes under the 1.5 °C and 2.0 °C warming levels with that in the reference period: all drought events (a), moderate droughts (b), severe droughts (c), and extreme severe droughts (d). Vertical lines denote ranges of the GCMs.

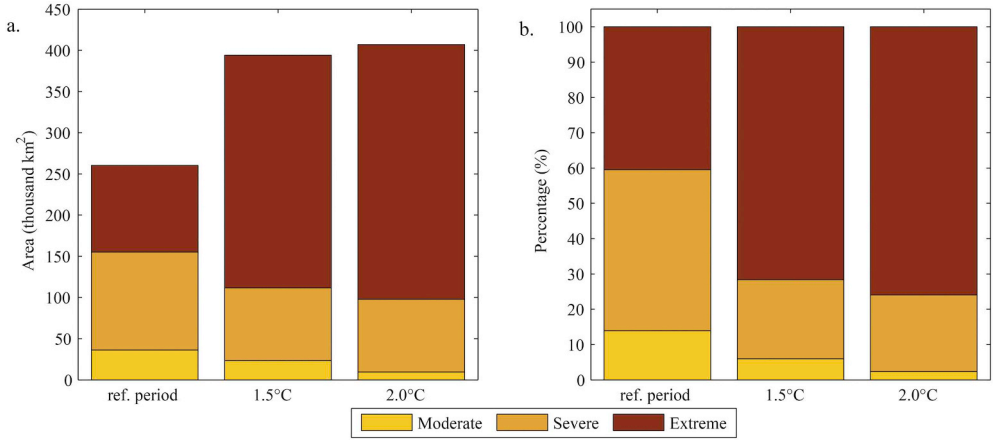

Fig. 9. Areal coverage of drought events with different magnitudes (a) and their percentages relative to total events (b) in the reference period and under the 1.5 °C and 2.0 °C warming levels.

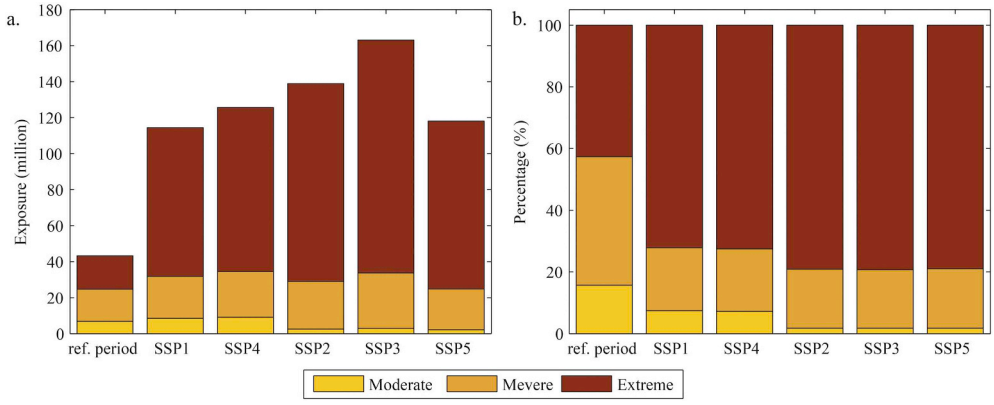

Fig. 10. Population exposed to droughts with different magnitudes (a) and their percentages (b) in the reference period and under the 1.5 °C and 2.0 °C warming levels.

SSP5, by which comparatively higher challenges of mitigation are expected in the future, based on the study of the impacts under the 2.0 °C warming scenario (Su et al., 2018).

It can be seen from Fig. 10 that the population exposed to droughts during the period 1986–2005 in the IRB amounted to approximately 43.2 million annually, which accounts for 22.8% of the total population. The percentages of people exposed to moderate, severe, and extreme severe droughts were 6.8, 18.0, and 18.4 million, respectively. Exposure to droughts in the future is assessed by the projected droughts and the predicted population based on SSPs. Under the 1.5 °C warming scenario, the population exposed to droughts under the sustainability pathway SSP1 might reach approximately 114.4 million per year, approximately 2.6-fold than that in the reference period. Based on SSP4, population exposure will be 125.7 million, about 11.3 million more than SSP1. The population exposed to moderate, severe, and extreme severe droughts will be 1.2-, 1.3-, and 4.5-fold than the reference period based on SSP1 and will be 1.3-, 1.4-, and 5.0-fold, respectively, based on SSP4. Under the 2.0 °C warming scenario, the population exposed to

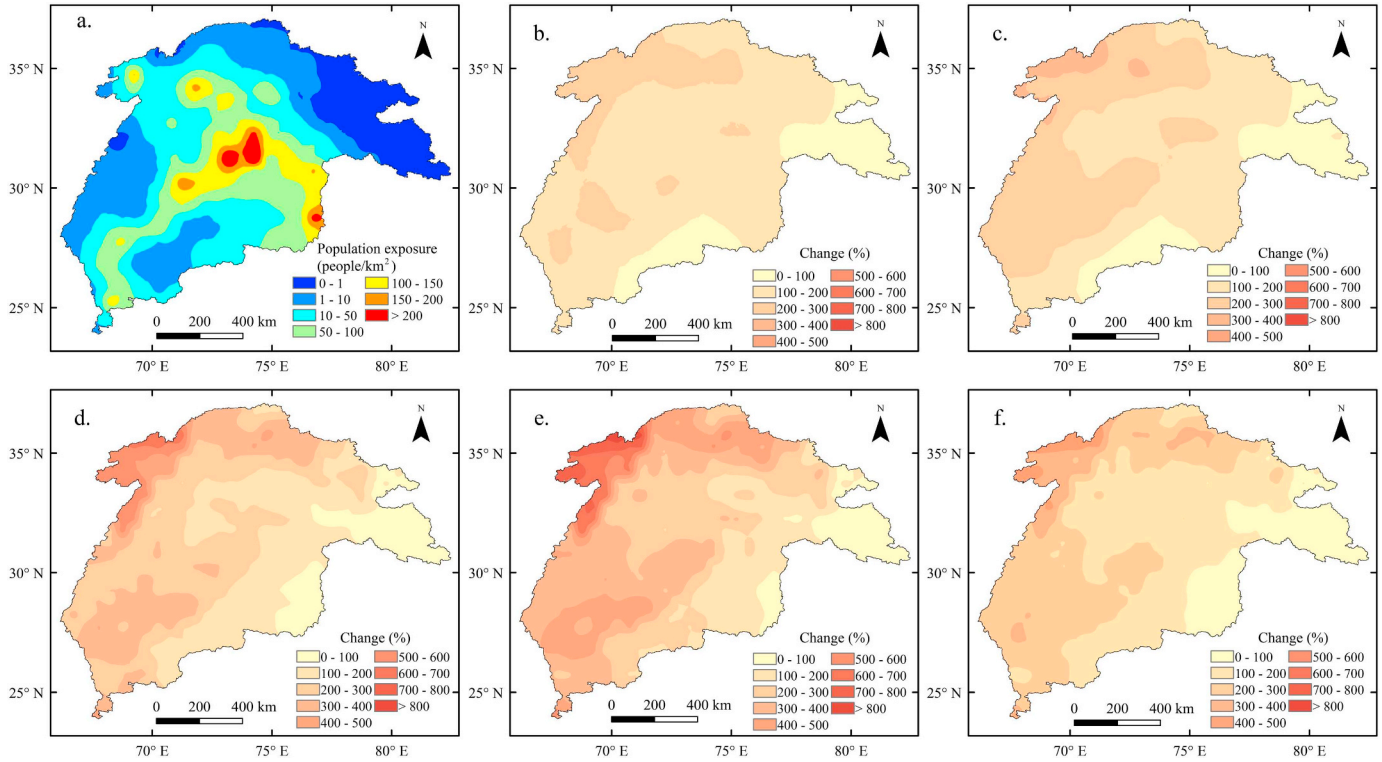

Fig. 11. Population exposure in 1986–2005 (a), changes in population exposure based on SSP1 and SSP4 at 1.5 °C warming relative to the reference period (b-c), and changes in population exposure based on SSP2, SSP3, and SSP5 at 2.0 °C warming relative to the reference period (d-f).

droughts will increase to 138.9 million per year in a continuation of the historical trend pathway SSP2. Based on the strongly fragmented pathway SSP3, population exposure will reach 163.1 million per year due to the strong increase in the population. In a growth-oriented world (SSP5), annual exposure is estimated as 118.1 million. The population exposed to moderate, severe, and extremely severe droughts based on SSP2, SSP3, and SSP5 will be 0.3–0.4-, 1.3–1.7-, and 5.1–7.0-fold, respectively, than that in the reference period.

Spatial distributions of population exposure in the IRB during the period 1986–2005 and under the 1.5 °C and 2.0 °C warming levels are compared in Fig. 11. In the reference period, drought exposure was approximately 39.3 per square kilometer averaged over the entire basin, and < 10 per square kilometer in the north, southeast and southwest, where the population density is low, but exceeded 100 per square kilometer in the central IRB, where the major cities in Pakistan, India, and Afghanistan (e.g., Islamabad, Lahore, Kabul, New Delhi, etc.) are concentrated.

Under the 1.5 °C warming scenario, spatial patterns of population exposure based on SSP1 and SSP4 will be similar to those in the reference period, but the exact numbers are comparatively higher. With relative to the reference period, population exposure will increase 1-fold in the central and eastern parts and 2-fold in the northwest IRB. Minimal exposure based on SSP1 and SSP4 can be expected in the upper IRB, while high exposure will occur in the central IRB. Due to the combined effects of increasing temperature and population, exposure to droughts under the 2.0 °C scenario will be higher than that under the 1.5 °C. Population exposure based on SSP2, SSP3, and SSP5 will remain low in the north but high in the central IRB. Based on SSP2, exposure in the northwestern IRB will increase > 4-fold compared with 1986–2005 and will increase 2- and 3-fold in the central and south IRB, respectively. The largest change will occur based on SSP3 in the northwestern IRB, with an increase of > 9-fold. Based on SSP5, exposure in the northwestern IRB will increase by > 3-fold, and that in the south IRB will increase by approximately 2-fold relative to the reference period. In the central and the eastern IRB, the increase will be < 2-fold.

5. Conclusion and discussion

Numerous studies have focused on changes in extreme events under global climate change (Hirabayashi et al., 2013; Huang et al., 2018). Currently, with the aim of maintaining global warming to 2.0 °C or 1.5 °C, socioeconomic impacts under different warming scenarios need to be further studied. Uncertainties still exist in estimation of drought exposure under climate change, which can be attributable to climate models, scenarios, indices, and the projected population (Maurer, 2007; Burke and J. Brown S., 2008; Kirono et al., 2011). In order to reduce uncertainties, we projected the frequency, intensity, and areal coverage of drought events in the Indus River Basin (IRB) based on multiple GCM outputs, and population exposure to droughts in the warming world was estimated using the predicted demographic condition under five SSPs. The main target of this paper is to provide regional evidence of the impacts resulting from an extra increase of 0.5 °C by assessing the effects of drought events so as to support policymakers to develop climate change adaptation and mitigation strategies.

With global warming, both precipitation and potential evapotranspiration are projected to increase in the IRB. The increase in annual precipitation will be 9.3 mm and 9.9 mm on average for the entire basin under the 1.5 °C and 2.0 °C warming levels, respectively, compared with 1986–2005. However, more obvious increases in potential evapotranspiration of 37.7 mm and 58.1 mm for the respective 1.5 °C and 2.0 °C warming levels are projected with relative to the reference period. A larger increase in potential evapotranspiration than in precipitation means that the water deficit might increase in the future, and droughts in the IRB will be aggravated, especially under the 2.0 °C warming scenario.

Compared with the reference period, drought frequency, intensity and areal coverage will increase by 35.9%, 19.5%, and 51.4%, respectively, under the 1.5 °C global warming. An additional 0.5 °C warming might lead to a further increase in drought frequency of 1.6%, as well as drought intensity and areal coverage of 4.4% and 3.3%, respectively. Although the total frequency and areal coverage of droughts

will increase, those of moderate and severe droughts will decrease with warming. The intensity of moderate and severe droughts in a warmer world will be similar to that of the reference period, but that of extreme severe droughts will increase. This means more drought events in the IRB can be expected with stronger intensity and larger coverage in the future.

It is clear that the population exposed to droughts in the IRB will increase greatly under every projected socioeconomic pathway. The exposure in the IRB was 43.2 million during the 1986–2005 period, of which, 6.8, 18.0, and 18.4 million were exposed to moderate, severe, and extreme severe droughts, respectively. Under 1.5 °C global warming, the population exposed to droughts will be 114.4 and 125.7 million based on SSP1 and SSP4, respectively. The percentage of the population exposed to moderate, severe, and extreme severe droughts will be 7.3–7.4%, 20.2–20.4%, and 72.2–72.5%, respectively. Population exposure will be 138.9, 163.1, and 118.1 million based on SSP2, SSP3, and SSP5, in response to the 2.0 °C warming level. The exposure to moderate, severe, and extreme severe droughts based on SSP2, SSP3, and SSP5 will be 0.3–0.4-, 1.3–1.7-, and 5.1–7.0-fold, respectively, than that of the 1986–2005 period.

Spatially, the population exposed to droughts will be similar to that in the reference period under the 1.5 °C and 2.0 °C scenarios, but with a higher quantity. The higher the temperature increase, the greater the exposure to droughts. Drought exposure will be low in the north and southeast, where the population density is scarce. High exposure will occur in the central IRB. Compared with the reference period, population exposure will increase significantly in the northwestern and southern regions. This implies that the plain area of the lower IRB will still have a high risk of droughts, and the risk of droughts in both the northwestern and northern IRB will increase greatly.

With increasing drought intensity, frequency, areal coverage, and expected population growth across the IRB, population exposure to droughts under the 1.5 °C and 2.0 °C global warming levels will be much higher than that in the reference period. Population exposure is projected to reach 163.1 million based on SSP3 in response to the 2.0 °C warming, i.e., 48.7 million more than the 114.4 million based on SSP1 in response to 1.5 °C warming. Maintaining the increase in the global average temperature to < 1.5 °C above the pre-industrial level can result in a 1.4-fold reduction in the population exposed to droughts in the IRB relative to the 2.0 °C warming.

A similar study on the population exposure to droughts in China under the 1.5 °C global warming scenario found that exposure to moderate droughts will be the largest compared with that of severe and extreme severe droughts (Chen et al., 2018). However, exposure to extreme severe droughts will be the largest in the IRB according to our analyses. This might be explained by the more intense increase in temperature in the IRB, which will lead to more severe drought events. Regarding to the spatial distribution of future population exposure to droughts in the IRB, our findings are consistent with those of Watts et al. (2015), i.e., exposure will be low in the mountains and desert areas but high in the plain area of the lower IRB.

Smirnov et al. (2016) analyzed the relative importance of climate change and demographic growth on future exposure to droughts under the RCP4.5 and RCP8.5 scenarios on a global scale and found that climate change will have a greater effect on increasing exposure than demographic change under both scenarios. This implies that climate change mitigation should be the main policy response in efforts to alleviate exposure to future extremes. For the world as a whole, plausible decreases in future population growth will not make a major dent in the significant increase of exposure during the remainder of this century. Increases in human exposure to future drought events will be a consequence of anthropogenic climate change. SSP1, which describes a world that shifts gradually but pervasively toward a more sustainable path, with a comparatively low future challenge of adaptation and mitigation, is the recommend path that should be pursued.

Acknowledgements

This study was jointly supported by the National Key R&D Program of China MOST (2017YFA0603701) and Joint project of the National Natural Science Foundation of China and the Pakistan Science Foundation (41661144027).

References

Aadhar, S., Mishra, V., 2017. High-resolution near real-time drought monitoring in South Asia. Sci. Data 4, 170145. https://doi.org/10.1038/sdata.2017.145.
Ahmad, S., Hussain, Z., Qureshi, A., 2004. Drought Mitigation in Pakistan: Current Status and Options for Future Strategies, Working Paper 85. International Water Management Institute, Colombo, Sri Lanka.
Andermann, C., Bonnet, S., Gloaguen, R., 2011. Evaluation of precipitation data sets along the Himalayan front. Geochem. Geophys. Geosyst. 12 (7), Q07023. https://doi.org/10.1029/2011GC003513.
Barthel, F., Neumayer, E., 2012. A trend analysis of normalized insured damage from natural disasters. Clim. Chang. 113 (2), 215–237.
Burke, E., J. Brown S., 2008. Evaluating uncertainties in the projection of future drought. J. Hydrometeorol. 9 (2), 292–299.
Byakatonda, J., Parida, B.P., Moalafhi, D.B., Kenabatho, P.K., 2018. Analysis of long term drought severity characteristics and trends across semiarid Botswana using two drought indices. Atmos. Res. 213, 492–508.
Chen, J., Gao, C., Zeng, X., et al., 2017. Assessing changes of river discharge under global warming of 1.5°C and 2°C in the upper reaches of the Yangtze River Basin: Approach by using multiple- GCMs and hydrological models. Quat. Int. 453, 63–73.
Chen, J., Liu, Y., Pan, T., et al., 2018. Population exposure to droughts in China under the 1.5 °C global warming target. Earth System Dyn. 9 (3), 1097–1106.
Deo, R.C., Sahin, M., 2015. Application of the Artificial Neural Network model for prediction of monthly Standardized Precipitation and Evapotranspiration Index using hydrometeorological parameters and climate indices in eastern Australia. Atmos. Res. 161 (Supplement C), 65–81.
Deo, R.C., Kisi, O., Singh, V.P., 2017. Drought forecasting in eastern Australia using multivariate adaptive regression spline, least square support vector machine and M5Tree model. Atmos. Res. 184 (Supplement C), 149–175.
Ghajarnia, N., Liaghat, A., Arasteh, P.D., 2015. Comparison and evaluation of high resolution precipitation estimation products in Urmia Basin-Iran. Atmos. Res. 158, 50–65.
Harris, I., Jones, P.D., Osborn, T.J., Lister, D.H., 2014. Updated high-resolution grids of monthly climatic observations - the CRU TS3.10 Dataset. Int. J. Climatol. 34 (3), 623–642.
He, B., Lv, A., Wu, J., Zhao, L., Liu, M., 2011. Drought hazard assessment and spatial characteristics analysis in China. J. Geogr. Sci. 21 (2), 235–249.
Hempel, S., Frieler, K., Warszawski, L., Schewe, J., Piontek, F., 2013. A trend-preserving bias correction — the ISI-MIP approach. Earth System Dyn. 4 (2), 219–236.
Hirabayashi, Y., Mahendran, R., Koirala, S., et al., 2013. Global flood risk under climate change. Nat. Clim. Chang. 3 (9), 816–821.
Huang, J., Wang, Y., Fischer, T., et al., 2017. Simulation and projection of climatic changes in the Indus River Basin, using the regional climate model COSMO-CLM. Int. J. Climatol. 37 (5), 2545–2562.
Huang, J., Zhai, J., Jiang, T., et al., 2018. Analysis of future drought characteristics in China using the regional climate model CCLM. Clim. Dyn. 50 (1), 507–525.
Hulme, M., 2016. 1.5 °C and climate research after the Paris Agreement. Nat. Clim. Chang. 6, 222.
IPCC (Intergovernmental Panel on Climate Change), 2013. Summary for Policymakers. Climate Change 2013: The Physical Science Basis. Contribution of Working Group I to the Fifth Assessment Report of the Intergovernmental Panel on Climate Change, Eds Stocker TF, Et al. Cambridge Univ Press, Cambridge, UK.
Hoegh-Guldberg, O., Taylor, D.Jacob.M., et al., 2018. Impacts of 1.5 °C Global Warming on Natural and Human Systems. In: Masson-Delmotte, V., Zhai, P., Portner, H.O. (Eds.), Global warming of 1.5 °C. An IPCC Special Report on the impacts of global warming of 1.5 °C above pre-industral levels and related global response to the threat of climate change, sustainalbe developement, and efforts to eradicate poverty, . https://www.ipcc.ch/site/assets/uploads/site/2/2018/SR15_Chapter3_Low_Res.pdf.
Kc, S., Lutz, W., 2017. The human core of the shared socioeconomic pathways: Population scenarios by age, sex and level of education for all countries to 2100. Glob. Environ. Chang. 42 (1), 181–192.
Kelley, C.P., Mohtadi, S., Cane, M.A., Seager, R., Kushnir, Y., 2015. Climate change in the Fertile Crescent and implications of the recent Syrian drought. Proc. Natl. Acad. Sci. U. S. A. 112 (11), 3241–3246.
King, A.D., Karoly, D.J., Henley, B.J., 2017. Australian climate extremes at 1.5 °C and 2 °C of global warming. Nat. Clim. Chang. 7, 412–416.
Kirono, D.G.C., Kent, D.M., Hennessy, K.J., Mpelasoka, F., 2011. Characteristics of Australian droughts under enhanced greenhouse conditions: results from 14 global climate models. J. Arid Environ. 75 (6), 566–575.
Maurer, E.P., 2007. Uncertainty in hydrologic impacts of climate change in the Sierra Nevada, California, under two emissions scenarios. Clim. Chang. 82 (3–4), 309–325.
Mishra, A.K., Singh, V.P., 2010. A review of drought concepts. J. Hydrol. 391 (1–2), 204–216.
Mishra, V., Aadhar, S., Asoka, A., Pai, S., Kumar, R., 2016. On the frequency of the 2015 monsoon season drought in the Indo-Gangetic Plain. Geophys. Res. Lett. 43 (23), 12102–12112.

Mitchell, D., James, R., Forster, P.M., et al., 2016. Realizing the impacts of a 1.5 °C warmer world. Nat. Clim. Chang. 6, 735–737.
O'Neill, B.C., Kriegler, E., Riahi, K., et al., 2014. A new scenario framework for climate change research: the concept of shared socioeconomic pathways. Clim. Chang. 122 (3), 387–400.
O'Neill, B.C., Kriegler, E., Ebi, K.L., et al., 2017. The roads ahead: Narratives for shared socioeconomic pathways describing world futures in the 21st century. Global Environ. Change Human Policy Dimensions 42, 169–180.
Rajbhandari, R., Shrestha, A., Kulkarni, A., Patwardhan, S., Bajracharya, S., 2014. Projected changes in climate over the Indus river basin using a high resolution regional climate model (PRECIS). Clim. Dyn. 44 (1–2), 339–357.
Schilling, J., Vivekananda, J., Nisha, P., Khan, M., 2013. Vulnerability to Environmental Risks and Effects on Community Resilience in Mid-West Nepal and South-East Pakistan. Environ. Nat. Resour. Res. 3 (4), 27–45.
Schleussner, C.-F., Lissner, T.K., Fischer, E.M., et al., 2016a. Differential climate impacts for policy-relevant limits to global warming: the case of 1.5°C and 2°C. Earth System Dyn. 7 (2), 327–351.
Schleussner, C.-F., Rogelj, J., Schaeffer, M., et al., 2016b. Science and policy characteristics of the Paris Agreement temperature goal. Nat. Clim. Chang. 6, 827–835.
Sheffield, J., Wood, E.F., 2007. Characteristics of global and regional drought, 1950–2000: Analysis of soil moisture data from off-line simulation of the terrestrial hydrologic cycle. J. Geophys. Res. Atmos. 112 (D17), 259–262.
Smirnov, O., Zhang, M.H., Xiao, T.Y., et al., 2016. The relative importance of climate change and population growth for exposure to future extreme droughts. Clim. Chang. 138 (1–2), 41–53.
Su, B., Huang, J., Gemmer, M., et al., 2016. Statistical downscaling of CMIP5 multi-model ensemble for projected changes of climate in the Indus River Basin. Atmos. Res. 178, 138–149.
Su, B., Jian, D., Li, X., et al., 2017. Projection of actual evapotranspiration using the COSMO-CLM regional climate model under global warming scenarios of 1.5°C and 2.0°C in the Tarim River basin, China. Atmos. Res. 196, 119–128.
Su, B., Huang, J., Fischer, T., et al., 2018. Drought losses in China might double between the 1.5 °C and 2.0 °C warming. Proc. Natl. Acad. Sci. 115 (42), 10600–10605.
Sun, H., Wang, Y., Chen, J., et al., 2017. Exposure of population to droughts in the Haihe River Basin under global warming of 1.5 and 2.0 °C scenarios. Quat. Int. 453, 74–84.
Sun, H., Wang, A., Zhai, J., et al., 2018. Impacts of global warming of 1.5°C and 2.0°C on precipitation patterns in China by regional climate model (COSMO-CLM). Atmos. Res. 203, 83–94.
Tobler, W., Deichmann, U., Gottsegen, J., Maloy, K., 1997. World population in a grid of spherical quadrilaterals. Int. J. Popul. Geogr. 3 (3), 203–225.
Trenberth, K.E., Dai, A.G., Van Der Schrier, G., et al., 2014. Global warming and changes in drought. Nat. Clim. Chang. 4 (1), 17–22.
UNFCCC, 2015. Conference of the Parties. Adoption of the Paris Agreement, Paris, pp. 1–32.
Van Vuuren, D.P., Kriegler, E., O'Neill, B.C., et al., 2014. A new scenario framework for climate change research: scenario matrix architecture. Clim. Chang. 122 (3), 373–386.
Vicente-Serrano, S.M., Begueria, S., Lopez-Moreno, J.I., 2010. A multiscalar drought index sensitive to global warming: the Standardized Precipitation Evapotranspiration Index. J. Clim. 23 (7), 1696–1718.
Warszawski, L., Frieler, K., Huber, V., et al., 2014. The Inter-Sectoral Impact Model Intercomparison Project (ISI-MIP): project framework. Proc. Natl. Acad. Sci. U. S. A. 111 (9), 3228–3232.
Watts, N., Adger, W.N., Agnolucci, P., et al., 2015. Health and climate change: policy responses to protect public health. Lancet 386 (10006), 1861–1914.
Xu, K., Yang, D., Yang, H., et al., 2015. Spatio-temporal variation of drought in China during 1961–2012: a climatic perspective. J. Hydrol. 526, 253–264.
Yatagai, A., Kamiguchi, K., Arakawa, O., et al., 2012. APHRODITE constructing a long-term daily gridded precipitation dataset for Asia based on a dense network of rain Gauges. Bull. Am. Meteorol. Soc. 93 (9), 1401–1415.
Zhai, J., Huang, J., Su, B., et al., 2016. Intensity–area–duration analysis of droughts in China 1960–2013. Clim. Dyn. 48 (1–2), 151–168.
Zhang, W., Zhou, T., Zou, L., Zhang, L., Chen, X., 2018. Reduced exposure to extreme precipitation from 0.5 °C less warming in global land monsoon regions. Nat. Commun. 9 (1), 3153. https://doi.org/10.1038/s41467-018-05633-3.